J. Phys. B: At. Mol. Opt. Phys. **21** (1988) 1055-1082. Printed in the UK

Ionisation cross sections of rare-gas atoms by electron impact

E Krishnakumar† and S K Srivastava

Jet Propulsion Laboratory, California Institute of Technology, Pasadena, CA 91109, USA

Received 22 June 1987, in final form 23 November 1987

Abstract. Normalised values of partial ionisation cross sections for the rare gases (He^+, Ne^+-Ne^{3+}, Ar^+-Ar^{3+}, Kr^+-Kr^{4+} and Xe^+-Xe^{5+}) have been measured from threshold to 1000 eV using a pulsed electron beam and ion extraction technique. The cross sections have been obtained for the singly ionised species by normalising the relative data with the results of Rapp and Englander-Golden below the onset of production of the doubly ionised species. These cross sections for the singly ionised species have then been used to calibrate the mass transmission efficiency of the ion extraction + analyser + detection system by the relative flow technique. The mass transmission curve thus obtained has been employed to determine the absolute cross sections of the multiply ionised species. Summation of the individual partial cross sections with proper weighting for charge is employed to obtain the total ion cross sections. The measured partial cross sections are fitted to an empirical formula for the ease of future use.

1. Introduction

The importance of the electron impact ionisation cross section data for atoms, molecules and other species like ions and radicals has long been realised. The data are of particular value to plasma physics, planetary physics and astrophysics.

Even though different types of experimental arrangements hae been designed and measurements have been reported both for total ionisation and partial ionisation cross sections of various species, accurate data for most of the species over a wide electron energy range are still not available. This has been due to the inherent complexities in apparently simple experiments and has been discussed by Kieffer and Dunn (1966). They made a compilation and critical evaluation of absolute cross sections up to 1966 for ionisation by electron impact on atoms and molecules and have presented the criteria for making accurate measurements. Recent reviews by Märk (1982, 1985) have highlighted the importance and intricacies (both theoretical and experimental) of obtaining accurate ionisation data.

Ionisation cross section data on rare gases have been more forthcoming compared with most of the other species. This has been due to their simple physical and chemical properties. Even then a survey of the literature for accurate data on them shows that the data are far from complete, particularly in the case of partial ionisation cross sections.

Total ionisation cross sections for the rare gases have been reported by various authors at a wide spectrum of energies and are listed in table 1. Of these there are four groups: (i) Smith (1930), (ii) Rapp and Englander-Golden (1965), (iii) Schram

† NRC-NASA resident Research Associate.

0953-4075/88/061055+28$02.50

Table 1. Gross ionisation cross sections.

Authors	Species	Energy range (eV)
Smith (1930)	He, Ne, Ar	Threshold-4500
Tozer and Craggs (1960)	Ar, Kr, Xe	Threshold-100
Asundi and Kurepa (1963)	He, Ne, Ar, Kr, Xe	Threshold-100
Rapp and Englander-Golden (1965)	He, Ne, Ar, Kr, Xe	Threshold-1000
Schram *et al* (1965)	He, Ne, Ar, Kr, Xe	600-20 000
Schram *et al* (1966a, b)	He, Ne, Ar, Kr, Xe	Threshold-600
Srinivasan and Rees (1967)	Ar	Threshold-100
Gaudin and Hagemann (1967)	He, Ne, Ar	100-2000
Fletcher and Cowling (1973)	He, Ne, Ar	Threshold-500
Kurepa *et al* (1974)	Ar	19-200
Wetzel *et al* (1987)	He, Ne, Ar, Kr, Xe	Threshold-200

et al (1965, 1966a, b) and (iv) Gaudin and Hagemann (1967) who have studied the gases in a fairly wide range (0 to 1000 eV) and there are serious disagreements among them. Keiffer and Dunn (1966) compared the data of Smith (1930) and Rapp and Englander-Golden (1965) and concluded that Smith's measurements could have suffered from systematic errors due to increase in path lengths of the electrons. De Heer and Inokuti (1985) point out that in the case of Ar the descrepancy in the above two measurements cannot be explained in terms of the path length effect, and conclude that much of the difference could be due to the error in the pressure measurement of Smith's experiment. They ascribe the similar differences in the measurements by Tozer and Craggs (1960) and Asundi and Kurepa (1963) from that of Rapp and Englander-Golden to the error in pressure measurements.

A comparison of the results of Schram *et al* (1965, 1966a, b) with those of Rapp and Englander-Golden (1965) shows a systematic difference in the cross section as a function of the mass of the atoms studied as well as the electron energy. In the case of He, Ne and Ar the results of Schram *et al* (1965, 1966a, b) are lower than that of Rapp and Englander-Golden (1965), the difference increasing with increasing energy. In the case of Kr the cross section of Schram *et al* (1965, 1966a, b) starts off at a higher value than that of Rapp and Englander-Golden (1965) at 100 eV. It is about the same at 150 eV and decreases faster as the energy increases. In the case of Xe the values of the cross section given by Schram *et al* (1965, 1966a, b) are higher throughout the energy range up to 1000 eV than that of Rapp and Englander-Golden (1965), with the percentage difference decreasing with increasing energy. Thus it is seen that apart from the absolute numbers which differ as a function of mass there is also a systematic difference in the realtive shapes of the cross section curves.

Gaudin and Hagemann (1967) have measured the partial and total ionisation cross section for He, Ne and Ar in the energy range of 100-2000 eV. Their data on neon lie between those of Rapp and Englander-Golden and Schram *et al* and the helium and argon data are lower than those of the above two groups.

Fletcher and Cowling (1973) measured the cross sections of He, Ne and Ar up to 500 eV and found that they are in close agreement with that of Rapp and Englander-Golden (1965). The measurements by Srinivasan and Rees (1967) up to 100 eV and Kurepa *et al* (1974) up to 200 eV were carried out to specifically eliminate the systematic errors, especially those from the pressure measurements conducted with a McLeod gauge. The distinctive feature of the measurement of Rapp and Englander-Golden

was the use of the gas flow method to determine the pressure instead of a McLeod gauge. Using a Tate and Smith (1932) apparatus similar to that employed by Asundi and Kurepa (1963) and using a McLeod gauge to determine the pressure employing a necessary correction Srinivasan and Rees measured the cross section for argon up to 100 eV. They obtained cross sections which are in very good agreement with those of Rapp and Englander-Golden (1965). The measurement of Kurepa *et al* (1974) employed the gas flow technique to measure pressure as done by Rapp and Englander-Golden (1965) instead of a McLeod gauge as used by other workers. After careful calibrations of the target-gas pressure and temperature as well as collection length Kurepa *et al* (1974) measured the cross sections for Ar from 19 to 200 eV and found them to be in close agreement with those of Rapp and Englander-Golden (1965), thus concluding that the experiments which employed the McLeod gauge suffered from the systematic error in pressure measurement unless corrected properly. Unfortunately both the measurements by Fletcher and Cowling (1973) and Kurepa *et al* (1974) which support the measurements of Rapp and Englander-Golden (1965) were not carried out for all the rare-gas species, and in a wider range of energies. The recent results of Montague *et al* (1984) on helium using a fast-atom-beam technique are in very good agreement with those of Rapp and Englander-Golden. More recently Wetzel *et al* (1987) have measured the partial cross sections of He, Ne, Ar, Kr and Xe up to 200 eV using a fast-atom beam and by summing up the partial cross sections with proper weight obtained the total cross sections. Their results are in good agreement with those of Rapp and Englander-Golden except in the case of Xe. For Xe they are higher by about 12% than that reported by Rapp and Englander-Golden and have tried to explain the difference in terms of the possible error in the latters' measurement of xenon pressure.

The partial ionisation cross sections of the rare gases have been measured by various authors and are summarised in table 2. Apart from the problems encountered in the measurement of total ionisation cross sections, partial ionisation cross section measurements have been faced with additional difficulties resulting from mass-to-charge-ratio dependence of the ion collecting, dispersing and detecting instruments. Märk (1982) has reviewed the partial ionisation cross section measurements with particular emphasis on the low-energy region.

The earliest quantitative measurements on the partial ionisation cross sections were reported by Bleakney (1930), Tate and Smith (1934) and Bleakney and Smith (1936). Most of these earlier measurements were carried out without proper calibration of the ion collecting optics, the mass spectrometers for dispersing the various ions and the detector and hence are unreliable. A look at table 2 shows that there is no partial cross section measurement reported for Kr and Xe in a single experiment from threshold to 1000 eV. In fact from 200 to 500 eV there is no measurement at all for Kr and Xe except those by Tate and Smith (1934) and Fox (1959, 1960). Also, the cross sections for the multiply ionised species (especially charge greater than 3+) have been measured by very few workers.

We have carried out the measurements using a pulsed electron beam and ion extraction technique. This technique was used for the electron impact ionisation studies as long ago as 1955 (Fox *et al* 1955) and was again employed by Foner and Nall (1961). We find that this technique when properly used can ensure a complete collection of all the ions produced in the collision region without disturbing the electron beam. This can also help in eliminating a possible ion trapping effect which can cause distortions in the excitation function curves. The technique is especially useful for the

Table 2. Partial ionisation cross sections.

Authors	Species	Energy range (eV)
Bleakney (1930)	He^+, Ne^+-Ne^{3+}, Ar^+-Ar^{4+}	Threshold-500
Bleakney and Smith (1936)	He^{2+}	Threshold-500
Tate and Smith (1934)	Kr^+-Kr^{4+}	Threshold-500
	Xe^+-Xe^{6+}	Threshold-600
Stevenson and Hipple (1942)	Ne^+, Ne^{2+}, Ar^+, Ar^{2+}	Threshold-200
Fox (1959)	He^+, He^{2+}	Threshold-400
	Xe^+-Xe^{7+}	Threshold-600
Fox (1960)	Ar^+-Ar^{4+}, Kr^+-Kr^{6+}	Threshold-600
Fiquet-Fayard (1962)	Ar^+-Ar^{5+}	Threshold-500
Fiquet-Fayard and Lahmani (1962)	Ar^+-Ar^{5+}	Threshold-500
Ziesel (1965)	Ne^+-Ne^{4+}	250-2000
Schram *et al* (1966)	He^+, He^{2+}, Ne^+-Ne^{5+}	500-16 000
Schram (1966)	Ar^+-Ar^{7+}	500-18 000
	Kr^+-Kr^{9+}, Xe^+-Xe^{13+}	500-15 000
Adamczyk *et al* (1966)	He^+, He^{2+}, Ne^+-Ne^{3+}	Threshold-2000
Ziesel (1967)	Kr^+-Kr^{5+}	Threshold-500
Gaudin and Hagemann (1967)	He^+, He^{2+}, Ne^+-Ne^{4+}, Ar^+-Ar^{5+}	100-2000
Van der Wiel *et al* (1969)	He^+, He^{2+}, Ne^+-Ne^{4+}, Ar^+-Ar^{6+}	2000-16 000
El-Sherbini *et al* (1970)	Kr^+-Kr^{6+}, Xe^+-Xe^{6+}	2000-14 000
Okudaira *et al* (1970)	Ar^+-Ar^{5+}	Threshold-1000
Crowe *et al* (1972)	Ar^+, Ar^{2+}	Threshold-300
Nagy *et al* (1980)	He^+, He^{2+}, Ne^+-Ne^{3+} Ar^+-Ar^{3+}, Kr^+-Kr^{3+}, Xe^+-Xe^{3+}	500-5000
Stephan *et al* (1980)	He^+, He^{2+}, Ne^+-Ne^{3+}, Ar^+-Ar^{3+}, Kr^+-Kr^{4+}	Threshold-180
Stephan and Mark (1984)	Xe^+-Xe^{3+}	Threshold-180
Mathur and Badrinathan (1984)	Ar^+-Ar^{2+}, Kr^+-Kr^{3+}	Threshold-200
Montague *et al* (1984)	He^+	Threshold-750
Mathur and Badrinathan (1985)	Xe^+	Threshold-150
Wetzel *et al* (1987)	He^+, Ne^+, Ar^+, Ar^{2+}, Kr^+-Kr^3, Xe^+-Xe^{3+}	Threshold-200

study of dissociative ionisation where fragment ions are produced with sufficient kinetic energies to defy collection by weak ion extraction electric fields. In addition, we have used the relative flow technique to calibrate the mass transmission efficiency of the ion collector+analyser+detector system to determine the partial ionisation cross sections of the multiply charged ions. This is the first time such a calibration has been used to obtain the cross sections of the multiply charged rare-gas ions. Also, this is the first time the partial cross sections from threshold to 1000 eV have been measured in a single experiment for most of the rare gases.

For ease of handling and future use we have fitted the present cross sections to an empirical function (see Bell *et al* 1983) using a chi-square minimisation technique (Srivastava and Nguyen 1987).

2. Experimental arrangement and method

Part of the experimental arrangement has been discussed earlier (Orient and Srivastava 1983). The significant modifications are the pulsed electron gun and the pulsed ion extraction system as well as the extension of the electron energy range up to 1000 eV.

A schematic diagram of the modified experimental arrangement is shown in figure 1. In the following the various relevant features of the experimental arrangement and method are described.

2.1. Pulsed extraction system

It is known that as a result of dissociation many ionic fragments are born with a considerable amount of kinetic energy. In order to extract these species completely from the collision region and to focus them at the entrance aperture of a quadrupole mass spectrometer such as the one employed in our experimental set-up one needs a high extraction voltage between the grids shown in figure 1. Our calculations show that for our type of extraction system a field of about 50 V cm^{-1} or more is required for a complete collection of protons born with an energy of 5 eV and leaving the collision region isotropically. Thus, in general, one needs to apply a bias of 50 V cm^{-1} between the two extraction grids. In a conventional arrangement, as used previously by us (Orient and Srivastava 1983), the electron beam when it enters the collision region is affected by the steady bias of 50 V on the grids. In order to avoid this situation we used a pulsed method of extraction. It was first used by Fox *et al* (1955) and later by Foner and Nall (1961). It employs a pulsed electron gun (Khakoo and Srivastava 1984, Krishnakumar and Srivastava 1986) which produces well collimated pulses of electrons with rise times of the order of 10 ns and durations which can be varied from 100 ns to 1 μs or more. The procedure for extracting positive ions from the collision

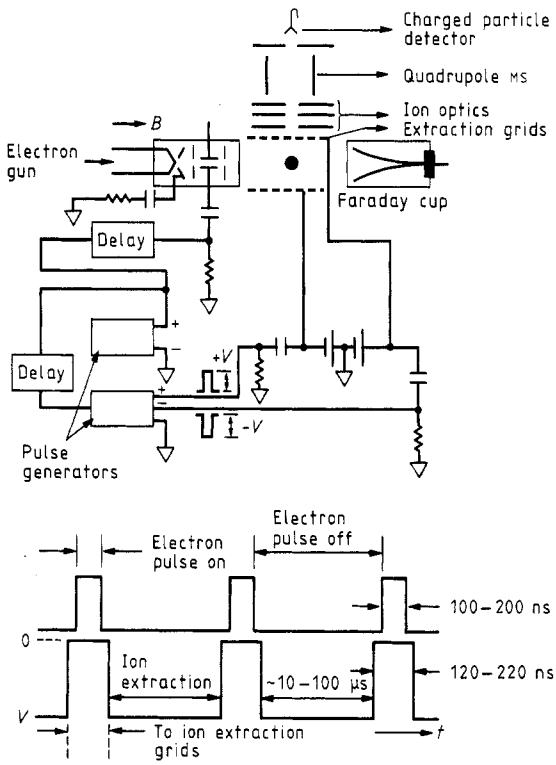

Figure 1. Schematic diagram of the experimental apparatus.

region was as follows. First, the extraction grid closest to the ion optics (figure 1) was biased by −50 V with respect to the ground. Then a +50 V pulse of width varying from 120 to 220 ns was applied to this grid. This brought the voltage on the extraction grid to zero (ground potential) during the time interval of the pulse width. A few ns later a pulse of about 5–10 V height and width varying from 100 to 200 ns (narrower in width than the pulse applied to the extraction grid) was applied to the electron gun. This enabled the electron gun to transmit to the collision region a collimated and pulsed beam of electrons. The ions resulting from the collision of electrons with the target species were collected and focused at the entrance aperture of the quadrupole mass spectrometer. This sequence of operation has two advantages: (i) it ensures a complete ion collection and (ii) the various ions born with different energies are transmitted through the ion optics with approximately the same efficiency.

2.2. *Ionisation efficiency curves*

The ionisation efficiency curves showing the variation of the relative ion intensity as a function of the electron impact energy for the various ionic species were obtained under the following conditions.

(*a*) The pulsed electron gun was operated at a time-averaged current of about 1 nA.

(*b*) The Faraday cup voltage was kept at +100 V throughout the measurements. It was previously determined that this voltage ensured the collection of all electrons without affecting the collision region.

(*c*) The collimating magnetic field was kept at about 100 G.

(*d*) The experiment could be done both with a crossed electron beam–molecular beam or with a static-gas target. In the crossed-beam mode the overlap volume (overlap of electron beam, atomic beam and the solid angle of the ion detector view cone) varied as a function of electron impact energy. To overcome this problem one can use a gas of known ionisation efficiency to calibrate the apparatus. We employed this method by using helium as the standard gas. The helium ionisation efficiency was taken as the one given by Bell *et al* (1983). This gave us reproducible results to within ±5%. Since this has the limitation of confining the energy range to the helium ionisation threshold at low energies and also the additional drawback of relying on the previously published helium data it was decided to make all ionisation efficiency measurements with a static-gas target. This provided us with reliable data on ionisation efficiency. A comparison of the static-gas measurements with those obtained by crossed beam in the available energy range showed an uncertainty of about ±5%, mostly at the low-energy region where the helium cross sections have the fast-rising edge. The static-gas data were reproducible to within ±3%. Careful tuning of the electron gun has recently provided us with results which are reproducible and consistent to within ±3% even in the crossed-beam mode.

(*e*) The ionisation efficiency curves were obtained by: (i) pulsing the electron gun and (ii) by the steady electron beam method. Since the ions of the rare-gas atoms are born with thermal energies the values of extraction voltages for the latter method were small (less than 10 V cm^{-1}) and the results of the two methods of extraction were identical.

2.3. *Determination of normalised values of cross sections and the mass transmission efficiency*

The ionisation efficiency curves represent the variation of the ion intensity as a function

of electron impact energy. However, this intensity is related to the ionisation cross section (in the crossed electron-beam–atomic-beam mode) through the following relation:

$$I(E_0) = K(m)\sigma(E_0) \int_v \rho(\boldsymbol{r}) \cdot f_e(\boldsymbol{r}, E_0) \cdot \Delta\Omega(\boldsymbol{r})\, \mathrm{d}\boldsymbol{r} \tag{1}$$

where $I(E_0)$ is the number of ions detected per second for incident electron energy E_0, $K(m)$ is an ion-mass-dependent factor which includes the combined efficiency of transmission of ions through the extraction grids, ion optics and quadrupole mass spectrometer and the detection efficiency of the charged particle detector $\rho(\boldsymbol{r})$ and $f_e(\boldsymbol{r}, E_0)$ are the target density and spatial electron flux distribution, respectively and $\mathrm{d}\Omega(\boldsymbol{r})$ is the solid angle of detection for a collision point located at $\boldsymbol{r}$ within the interaction region of the two beams.

It is clear from equation (1) that in order to obtain $\sigma(E_0)$ from the knowledge of $I(E_0)$ (experimentally measured) one has to determine the values of several unknown factors. In commonly used experimental conditions this is an almost impossible task. Therefore, one has to use some type of calibration technique for the determination of the unknown factors. For this purpose a relative flow technique was developed in the past and has been described in detail by Orient and Srivastava (1983). Briefly, the experimental arrangement (figure 1) utilises a capillary array to form an atomic or molecular beam. If the pressure behind the capillary array is low enough then the properties of the target beam such as spatial and velocity distribution of the atoms can be accurately predicted (Brinkmann and Trajmar 1981). The experimental procedure is as follows. First, a beam of He atoms (standard gas, S) or some such species whose cross sections are accurately known is made to flow through the capillary array under the conditions of molecular flow. The intensity of positive ions, $I_S(E_0)$, and the flow rate of the target gas F_S through the capillary array are recorded. Second, the standard gas is replaced by the gas under study whose cross sections are unknown. Again, the ion intensity $I_u(E_0)$ and flow rate F_u for this gas are noted. This operation is done in such a way that all the conditions such as the electron beam current remain the same. The ion intensities and cross sections for the two gases are related through the following relation (Srivastava *et al* 1975):

$$\sigma_u(E_0) = \sigma_S(E_0) \frac{I_u(E_0)}{I_S(E_0)} \left(\frac{m_S}{m_u}\right)^{1/2} \frac{F_S}{F_u} \frac{K(m_S)}{K(m_u)} \tag{2}$$

where E_0 is the kinetic energy of the colliding electron, $\sigma_u(E_0)$ and $\sigma_S(E_0)$ the cross sections for the ionisation of the respective species, m_u and m_S their respective molecular weights and $K(m_u)$ and $K(m_S)$ are the mass-dependent transmission and detection efficiencies of the experimental apparatus.

In (2) all the quantities, except the ratio $K(m_S)/K(m_u)$, are simple to measure. For obtaining this ratio we employed the cross sections of rare gases at electron impact energies of 200 and 500 eV determined by us by normalising our relative cross sections for singly ionised species to the data of Rapp and Englander-Golden (1965) at electron impact energies lying below the onset of double ionisation. For masses lying between the masses of rare-gas atoms we used interpolation by assuming that the ratio varies linearly with the mass. These ratios were then used to determine the relative values of multiply ionised species with respect to the singly ionised ones (e.g. $\sigma(Ar^{2+}, Ar^{3+})/\sigma(Ar^+)$) over the entire electron impact energy range from threshold to 1000 eV.

2.4. Total cross sections

The 'total cross sections can be obtained by summing the individual partial cross sections. If the particle-counting techniques are employed for measuring the partial cross sections then the sum of all partial ionisation cross sections gives the 'total counting ionisation cross section' $\sigma_c(T)$ and is given by

$$\sigma_c(T) = \sum_p \sigma_p + \sum_i \sigma_p^i \tag{3}$$

where σ_p is the cross section for single ionisation and σ_p^i is the partial ionisation cross section for the generation of double and multiply ionised species.

In the past most investigators have obtained total ionisation cross sections by measuring the total ionisation current. In this case, the cross section is defined as the 'total ionisation cross section' $\sigma_I(T)$ and is represented by the following relation:

$$\sigma_I(T) = \sum_p \sigma_p + \sum_i Z_i \sigma_p^i \tag{4}$$

where Z_i is the stage of ionisation.

Since most results on the total cross sections have been obtained by the second method we employed (4) for the calculation of $\sigma_I(T)$ and compared with the previous data.

2.5. Parametrisation of the cross section data

We have parametrised the cross section data for the modellers of the various plasmas. The method of parametrisation is same as that followed by Bell *et al* (1983). The details of this method are given by Srivastava and Nguyễn (1987). Briefly, the partial cross section can be represented by the following empirical formula:

$$\sigma_p(E) = \frac{1}{IE}\left[A \ln\left(\frac{E}{I}\right) + \sum_{i=1}^{N} B_i \left(1 - \frac{I}{E}\right)^i\right]. \tag{5}$$

where A and B_i are coefficients obtained by fitting to the experimental data, I is the ionisation potential, E is the electron impact energy and i determines the number of terms N needed to fit the experimental data. As a first approximation, the coefficient A can be calculated by fitting to the Bethe relation at high energies:

$$\sigma_p(E) = \frac{1}{IE}(A \ln(E) + B) \tag{6}$$

where B is a fitting constant obtained by fitting (6) to the data measured at high electron impact energies. The coefficient can also be obtained from the following relation:

$$A = \frac{1}{\pi\alpha}\int_I^{\alpha} \frac{\sigma_{ph}}{E}\, dE \tag{7}$$

where σ_{ph} is the photoionisation cross section for the species under investigation and α is the fine-structure constant.

For the fitting of data to (5) a χ^2 minimisation technique was employed and the details can be found in a book by Bevington (1969) or in a publication by Srivastava and Nguyễn (1987).

3. Errors and their estimation

The errors contributing to the final results can be separated into those involved in the relative shape measurement and those involved in the normalisation procedure and are described below.

3.1. Relative shape

The errors that could contribute to the relative shape measurement are from the electron current measurement, pressure measurement, path length change of electrons, and space charge effects and random errors including statistical errors from ion counting and the fitting procedures.

The electron current was measured by a Keithley 600A electrometer. The electron current varied by a factor of two in the energy range up to 1000 eV. The overall calibration error and the possible non-linearity of the electron current measurement is estimated to be about ±2%.

The entire electron energy was scanned within a time of 100 s which ensured that the experimental conditions did not change significantly during one complete scan. During this time there was very little change in the gas pressure/flow rate. This was determined by monitoring the ion counts at a particular electron energy and noting the change in counts with time. The uncertainty in the pressure was found to be better than 0.1% during one scan.

Since a pulsed electron beam and pulsed ion extraction was used there was no effect of the ion extraction voltage on the electron beam. This coupled with relatively low magnetic field (~100 G) and low pressure ($\sim 1 \times 10^{-7}$ Torr) eliminates any possible path length corrections. Non-linear effects in the ion extraction as a function of electron energy could develop if the electron current is large and/or the gas pressure is high giving rise to a large number of ions in the ionisation region. Either high electron current or high pressure or both could give rise to space charge and ion trapping effects which contribute to non-linear ion extraction as a function of the electron energy. Moreover since the experiment is done with the pulsed technique even smaller effects due to space charge are eliminated. We have measured any possible contribution from space charge effects by changing both the electron current and gas pressure in the ranges we used for the final measurements and found none.

The ion detection system has a linear counting rate up to 10^6 counts/s. In the present case the rate was about 5000 counts/s. The linearity in this range was also checked by counting separately the $Ne^+(20)$ and $Ne^+(22)$ ions and taking their ratios at different count rates. Thus the error due to the non-linearity of the ion detection system was practically zero.

Apart from the above-mentioned systematic errors there could be some random errors present due to statistical fluctuation of the counts and possible changes in the electron beam conditions when the data are collected over a large period of time. The errors from statistical fluctuation are reduced by collecting the data for sufficiently long duration. The error from this is negligible in the case of singly ionised species

but is a maximum of approximately 2% for species which have cross sections less than about one Mb. The changes in the electron beam conditions could be in its energy (due to possible variation in contact potentials) as well as possible spatial shifts due to changing filament conditions. The energy spread of the electron gun (~0.5 eV) and the step size (0.5 eV) used for scanning the energy range also could add to the uncertainty in the relative shpaes at or near the thresholds. The contribution due to changes in the electron beam conditions was found to be absent in subsequent measurements. But measurements separated by a month with changed focusing conditions of the gun showed a reproducibility of about ±3% and are taken as the upper limit for all random errors.

3.2. Normalised values of cross sections

Since the ionisation efficiency curves are reasonably fast rising in the energy range used for this purpose there could be an uncertainty resulting from this procedure. The uncertainty from this was calculated by taking the derivative of the cross section with respect to electron energy at the relevant energies for each of the species.

For measuring the ionisation efficiency the electron energy was advanced in 0.5 eV steps. The electron gun energy resolution is approximately 0.5 eV. The deviations in energy due to contact potentials were eliminated by matching the onset of the excitation function curves with the spectroscopic values of the appearance potential. The maximum uncertainty resulting from this procedure should be the sum of the energy width of the electron beam and the energy scanning step size. Thus the overall uncertainty will be a maximum of 1 eV in energy. The statistical error is about 1%. Thus the worst case error is about ±3.6% for Xe. For other species it is less. These along with the error in the relative shape and the estimated uncertainties in the measurement of Rapp and Englander-Golden (7%) should be the overall uncertainty in the absolute cross sections for the singly ionised species.

Table 3. Error estimates.

	% error	
Species	Relative shape	Absolute cross section
He^+	5	10
Ne^+	5	10
Ar^+	5	10
Kr^+	5	10
Xe^+	5	10
Ne^{2+}	6	13
Ne^{3+}	7	22
Ar^{2+}	6	13
Ar^{3+}	7	19
Kr^{2+}	6	14
Kr^{3+}	6	15
Kr^{4+}	7	14
Xe^{2+}	6	19
Xe^{3+}	6	21
Xe^{4+}	6	14
Xe^{5+}	7	13

For the multiply ionised species the contributions to the uncertainty in the absolute cross section will be from the relative shape and their normalisation procedure. The normalisation was carried out by measuring the mass transmission of the system using the singly ionised species by the relative flow technique. Most of the remaining uncertainties are from the random errors—statistical errors from the counting, the possible small fluctuations in the flow rate (including the measurement error) and the error resulting from fitting the mass transmission curve. Instead of evaluating all of these errors individually, we have determined the standard deviation from a number of measurements of the absolute cross sections. This, along with the uncertainty in the relative shape and the overall unceratinty in the respective singly ionised species, gives the total uncertainty in the normalised values of cross sections of the multiply ionised species. The overall uncertainty in the values of these cross sections for each species was determined by taking the square root of the sum of the squares of the individual uncertainties including the fitting errors. These are given in table 3 for each of the species.

4. Results

We have measured the partial ionisation cross sections for the rare gases He, Ne, Ar, Kr and Xe in the energy range from threshold to 1000 eV. These individual partial cross sections were summed up with proper weight for the degree of ionisation to obtain the total ionisation cross sections. The data are presented in figures 2–14. All

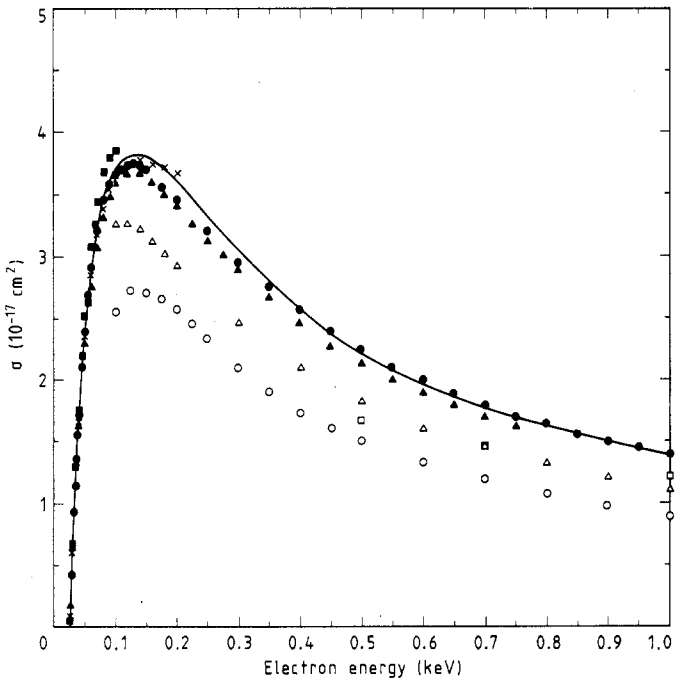

Figure 2. The total ionisation cross section for He as a function of electron energy. ■, Asundi and Kurepa (1963); ●, Rapp and Englander-Golden (1965); △, Schram *et al* (1965, 1966a, b); ○, Gaudin and Hagemann (1967); □, Nagy *et al* (1980); ▲, Montague *et al* (1984); ×, Wetzel *et al* (1987); full curve, present data. Some of these data, including the present are prepared assuming the He^{2+} cross section to be negligibly small. Not included in figure are the data by Smith (1930) and Fletcher and Cowling (1973) (see text).

Table 4. Coefficients obtained for fit to experimental data described by equation (5) in units of 10^{-18} cm^2 eV^2.

	A	B_1	B_2	B_3	B_4	B_5	B_6	B_7	B_8
Ne^{1+}	2.927499×10^{5}	-2.903135×10^{5}	-4.8969×10^{4}	-8.2398×10^{4}	-4.3983×10^{4}	5.3937×10^{5}	—	—	—
Ne^{2+}	1.28295×10^{4}	-6.7517×10^{3}	-8.66567×10^{4}	6.20247×10^{5}	-1.7617×10^{6}	2.77427×10^{6}	-1.4885×10^{6}	—	—
Ne^{3+}	3.4239×10^{3}	-1.83561×10^{3}	-1.2222×10^{4}	5.26827×10^{4}	7.1852×10^{4}	-1.09389×10^{5}	—	—	—
Ar^{+}	9.691×10^{4}	-2.1005×10^{5}	1.9536×10^{6}	-9.8279×10^{6}	2.6616×10^{7}	-3.2882×10^{7}	1.5184×10^{7}	—	—
Ar^{2+}	1.5907×10^{4}	-6.5172×10^{3}	1.2754×10^{5}	6.3048×10^{5}	-6.3411×10^{5}	—	—	—	—
Ar^{3+}	—	—	—	—	—	—	—	—	—
Kr^{1+}	4.1675×10^{5}	-4.0890×10^{5}	7.2968×10^{4}	-2.1400×10^{5}	2.2089×10^{5}	—	—	—	—
Kr^{2+}	7.5148×10^{4}	-6.0195×10^{4}	-4.0877×10^{5}	3.5519×10^{6}	-5.5391×10^{6}	2.4861×10^{6}	—	—	—
Kr^{3+}	1.4111×10^{5}	-1.2574×10^{5}	1.3456×10^{5}	-2.5639×10^{6}	1.3929×10^{7}	-3.0849×10^{7}	3.0046×10^{7}	-1.0569×10^{7}	—
Kr^{4+}	9.4224×10^{4}	-8.5056×10^{4}	-1.7799×10^{5}	9.4494×10^{5}	-2.9821×10^{6}	4.6540×10^{6}	-2.4490×10^{6}	—	—
Xe^{1+}	5.3180×10^{5}	-5.5272×10^{5}	4.3084×10^{5}	-1.0138×10^{6}	4.3057×10^{5}	—	—	—	—
Xe^{2+}	2.1693×10^{5}	-1.5897×10^{5}	1.4518×10^{6}	-2.8675×10^{7}	2.1184×10^{8}	-7.046×10^{8}	1.1679×10^{9}	-9.4364×10^{8}	2.9599×10^{8}
Xe^{3+}	2.2868×10^{5}	-3.2675×10^{5}	5.4044×10^{6}	-5.7805×10^{7}	2.5296×10^{8}	-4.9809×10^{8}	4.4934×10^{8}	-1.5182×10^{8}	—
Xe^{4+}	1.8596×10^{5}	-1.1909×10^{5}	8.7999×10^{5}	-1.2579×10^{7}	5.1209×10^{7}	-4.9345×10^{7}	-7.8086×10^{7}	1.6624×10^{8}	-7.8863×10^{7}
Xe^{5+}	9.4585×10^{4}	-4.0896×10^{4}	-7.5570×10^{5}	6.5717×10^{6}	-1.5531×10^{7}	1.4689×10^{7}	-4.8586×10^{6}	—	—

Table 5. Partial and total ionisation cross sections of He, Ne and Ar.

Energy (eV)	$\sigma(\times 10^{-18}\ \mathrm{cm}^2)$								
	He^+	Ne^+	Ne^{2+}	Ne^{3+}	Ne (total)	Ar^+	Ar^{2+}	Ar^{3+}	Ar (total)
1000	13.9	37.0	1.60	0.140	40.6	72.1	4.20	0.911	83.2
950	14.4	38.1	1.68	0.147	41.9	74.4	4.30	0.927	85.8
900	14.9	39.2	1.76	0.153	43.2	78.1	4.60	0.937	90.1
850	15.6	40.7	1.86	0.162	44.9	81.0	4.85	0.953	93.6
800	16.3	42.3	1.97	0.171	46.8	84.5	5.12	0.963	97.6
750	17.0	43.9	2.08	0.180	48.6	90.1	5.67	0.968	104.3
700	17.8	45.6	2.22	0.192	50.6	94.9	6.04	0.975	109.9
650	18.3	47.6	2.37	0.205	53.0	102.1	6.39	0.980	117.8
600	19.6	49.8	2.53	0.218	55.5	109.2	6.92	0.984	126.0
550	20.7	52.2	2.71	0.231	58.3	115.5	7.46	0.982	133.4
500	22.0	54.7	2.94	0.245	61.3	125.6	7.96	0.968	144.4
450	23.6	57.5	3.16	0.255	64.8	132.5	8.96	0.942	153.2
400	25.7	61.1	3.37	0.260	68.6	143.6	10.1	0.901	166.5
350	28.0	64.3	3.59	0.260	72.3	155.9	11.3	0.831	181.0
300	30.5	68.3	3.73	0.237	76.5	170.4	13.4	0.714	199.3
275	31.8	70.2	3.77	0.231	78.4	178.2	14.4	0.694	209.1
250	33.2	72.0	3.78	0.186	80.1	188.4	15.6	0.714	221.7
225	34.7	73.5	3.72	0.138	81.4	198.1	17.1	0.761	234.6
200	36.0	74.9	3.57	0.096	82.3	209.0	18.7	0.804	248.8
195	36.3	75.2	3.49	0.085	82.4	210.9	19.1	0.813	251.5
190	36.5	75.3	3.43	0.076	82.4	213.1	19.6	0.818	254.8
185	36.7	75.5	3.39	0.006	82.5	215.3	19.9	0.822	257.6
180	37.0	75.6	3.31	0.056	82.4	217.2	20.3	0.826	260.3
175	37.2	75.7	3.20	0.048	82.2	220.8	20.5	0.826	264.3
170	37.4	75.8	3.10	0.039	82.1	222.5	21.0	0.825	267.0
165	37.6	76.0	3.00	0.032	82.1	224.2	21.4	0.818	269.5
160	37.7	76.0	2.91	0.025	81.9	226.5	21.8	0.808	272.5
155	37.9	75.9	2.79	0.019	81.5	228.7	22.1	0.792	275.3
150	38.0	75.8	2.64	0.014	81.1	231.9	22.4	0.777	279.0
145	38.1	75.6	2.49	0.009	80.6	235.5	22.7	0.745	283.1
140	38.1	75.1	2.30	0.006	79.7	238.3	23.0	0.723	286.5
135	38.2	74.5	2.15	0.004	78.8	240.9	23.3	0.678	289.5
130	38.1	73.8	1.96	0.001	77.7	242.9	23.4	0.624	291.6
125	38.1	73.1	1.79	—	76.7	244.5	23.5	0.580	293.2
120	38.0	72.2	1.59	—	75.4	246.8	23.5	0.502	295.3
115	37.8	71.4	1.43	—	74.3	248.9	23.4	0.435	297.0
110	37.6	70.5	1.22	—	72.9	250.5	23.3	0.337	298.1
105	37.3	69.3	1.03	—	71.4	251.4	23.1	0.238	298.4
100	37.0	67.5	0.868	—	69.2	252.2	22.8	0.145	298.2
95	36.7	65.9	0.671	—	67.2	253.6	22.5	0.073	298.8
90	36.2	63.4	0.513	—	64.4	253.6	22.0	0.021	297.7
85	35.5	60.8	0.359	—	61.5	253.8	21.1	—	296.0
80	34.5	58.1	0.237	—	58.6	252.8	20.4	—	293.6
75	33.3	55.3	0.126	—	55.6	251.0	19.3	—	289.6
70	32.1	51.8	0.063	—	51.9	248.6	16.7	—	282.0
65	30.8	48.0	0.020	—	48.0	247.1	13.4	—	273.9
60	29.1	43.6	—	—	43.6	248.4	9.95	—	268.3
55	26.7	39.2	—	—	39.2	250.3	5.35	—	261.0
50	23.7	33.9	—	—	33.9	249.7	1.24	—	252.2
45	20.9	29.0	—	—	29.0	248.0	0.05	—	248.1
40	16.8	23.7	—	—	23.7	239.3	—	—	239.3
35	10.8	17.3	—	—	17.3	192.0	—	—	192.0
30	6.72	11.1	—	—	11.1	172.4	—	—	172.4
25	0.40	3.77	—	—	3.77	115.8	—	—	115.8
20	—	—	—	—	—	41.2	—	—	41.2
15	—	—	—	—	—	—	—	—	—

of them were fitted to an empirical formula (see §2.5). Since it has been established that most of the earlier measurements have suffered from systematic errors and lack of proper calibration procedures (Kieffer and Dunn 1966, Märk 1982) we have not included most of the measurements before 1965 for comparison with the present data, except in certain cases. Also for the sake of clarity of presentation we have omitted certain measurements (like Srinivasan and Rees 1967 and Fletcher and Cowling 1973) which are in very good agreement with the ones we have used for comparison. For making the comparisons we have evaluated the percentage deviation of each set of data with ours both in relative shape and absolute magnitude. In all cases, the percentage deviation of the absolute values has been calculated with respect to our data.

The fitting parameters derived for each ion species are given in table 4. The original data are presented in tables 5 and 6. The fitting parameters provide accurate values ($\simeq 5\%$) of cross sections for electron impact energies which are about 10 eV above the threshold for the appearance potential. In table 4 we have not presented these parameters for Ar^{3+}. This is due to the fact that we could not get a good fit for those data. This may be due to the fact that these cross sections are dominated by Auger processes.

In the following the results for each individual ionic species are discussed.

4.1. He

The data on He^+ are given in figure 2. They are compared with the total cross section data measured by other groups. It is assumed that in our measurements contributions of He^{2+} are negligible. The He^+ data are normalised with those of Rapp and Englander-Golden at 70 eV. The previously measured helium data show a wide spread. At 1000 eV, the cross section by Gaudin and Hagemann is off by as much as 36%, and that by Schram *et al* is 21% lower than that of Rapp and Englander-Golden. The recent measurement of Montague *et al* (1984) from threshold to 750 eV using a crossed electron–fast-atom-beam technique is in very close agreement with those of Rapp and Englander-Golden. The present data agree to within 4% with those of Rapp and Englander-Golden and to within 2% with those of Montague *et al* in relative shape over the entire electron impact energy range.

4.2. Ne

Ne^+ data are shown in figure 3 along with other reported measurements. Our data are higher than the previous measurements of Wetzel *et al* (1987) and Stephan *et al* (1980). However, they are well within the estimated uncertainties of all the experiments. The data of Schram *et al* (1966a, b) are lower than ours by as much as 23% at 1000 eV with the relative shape in the 500–1000 eV region agreeing within 3%. The results of Nagy *et al* (1980) are lower by about 21% at 1000 eV and differ in relative shape by about 7%. The results by Adamczyk *et al* (1966) (30–1000 eV) are lower than the present data by about 25–30% with the relative shapes agreeing within 5%. The measurements by Gaudin and Hagemann (1967) (100–1000 eV) are lower than ours by about 10–20% in absolute magnitude with the relative shape differing by about 10%.

The Ne^{2+} and Ne^{3+} results are given in figure 4 along with those reported by Stephan *et al* (1980), Nagy *et al* (1980), Gaudin and Hagemann (1967), Adamczyk *et al* (1966) and Schram *et al* (1966a, b). For Ne^{2+} measurements by Gaudin and Hagemann (100–1000 eV) are about 13% lower than our values except at low energies.

Table 6. Partial and total ionisation cross sections of Kr and Xe.

Energy (eV)	$\sigma(\times 10^{-18}\ \mathrm{cm}^2)$										
	Kr^+	Kr^{2+}	Kr^{3+}	Kr^{4+}	Kr (total)	Xe^+	Xe^{2+}	Xe^{3+}	Xe^{4+}	Xe^{5+}	Xe (total)
1000	105.0	7.50	4.27	1.21	137.7	140.0	16.2	8.61	3.98	1.14	219.9
950	111.0	7.80	4.43	1.24	144.9	144.3	16.5	8.95	4.04	1.17	226.2
900	113.5	8.10	4.59	1.26	148.5	149.7	16.9	9.31	4.12	1.19	233.9
850	119.2	8.59	4.72	1.28	155.7	156.7	17.0	9.85	4.20	1.22	243.2
800	123.8	8.91	4.86	1.31	161.4	161.3	17.8	10.2	4.33	1.26	251.1
750	129.4	9.19	4.95	1.35	168.0	165.9	18.4	10.7	4.42	1.28	258.9
700	135.2	9.55	5.09	1.35	175.0	172.8	19.3	11.2	4.56	1.30	269.7
650	140.9	9.90	5.20	1.37	181.8	179.8	19.8	11.6	4.67	1.35	279.6
600	148.5	10.5	5.32	1.37	190.9	189.0	20.7	12.0	4.82	1.39	292.6
550	157.2	11.1	5.46	1.36	201.2	198.2	21.4	12.6	5.03	1.45	306.2
500	165.6	11.8	5.52	1.32	211.0	211.1	22.4	13.2	5.23	1.49	323.9
450	178.9	12.7	5.52	1.26	225.9	223.5	23.5	13.9	5.48	1.51	341.7
400	192.6	13.9	5.48	1.14	241.4	239.7	24.9	14.5	5.63	1.53	363.2
350	209.4	15.2	5.36	0.979	259.8	258.1	26.3	15.1	5.71	1.55	386.6
300	229.2	17.3	5.18	0.729	282.3	282.1	27.9	15.8	5.93	1.47	416.4
275	239.8	18.7	5.06	0.610	294.8	295.5	29.0	16.0	6.20	1.26	432.6
250	253.2	20.2	4.88	0.448	310.0	309.7	30.6	16.4	6.54	0.984	451.2
225	267.2	22.1	4.64	0.310	326.7	326.5	32.7	17.1	6.60	0.604	472.6
200	282.9	24.1	4.44	0.177	345.1	344.3	35.2	18.7	6.05	0.225	496.1
195	276.4	24.4	4.39	0.154	359.0	346.5	36.1	18.9	5.76	0.152	499.2
190	289.8	25.0	4.34	0.132	353.3	349.8	37.0	19.3	5.35	0.109	503.6
185	292.5	25.4	4.28	0.112	356.6	353.1	38.0	19.6	4.85	0.006	507.6
180	296.3	26.0	4.21	0.097	361.3	356.7	38.9	20.1	4.46	0.038	512.8
175	300.8	26.4	4.18	0.081	366.5	360.9	39.9	20.7	3.88	0.017	518.4
170	303.2	26.9	4.00	0.065	369.3	365.4	41.0	21.1	3.45	—	524.5
165	307.3	27.4	3.83	0.049	373.8	370.1	42.1	21.5	2.98	—	530.7
160	310.0	28.0	3.66	0.035	377.1	374.8	43.5	22.1	2.44	—	537.9
155	313.4	28.6	3.56	0.026	381.4	379.2	44.7	22.8	2.08	—	545.3
150	317.1	29.4	3.45	0.015	386.3	387.2	46.0	23.3	1.73	—	556.0
145	321.8	29.8	3.37	0.011	391.6	392.4	47.5	23.9	1.40	—	564.7
140	325.1	30.3	3.23	0.005	395.4	396.8	49.3	24.0	1.08	—	571.7
135	329.7	31.2	3.07	0.0015	401.3	402.5	50.7	23.9	0.934	—	579.3
130	333.9	31.8	2.28	—	406.0	407.5	52.5	23.4	0.718	—	585.6
125	338.0	32.5	2.62	—	410.9	414.8	53.6	22.2	0.503	—	590.6
120	342.9	33.2	2.25	—	416.1	419.1	54.4	20.4	0.288	—	590.3
115	346.6	33.8	1.96	—	420.1	424.9	54.8	18.3	0.144	—	590.0
110	350.1	34.2	1.55	—	423.2	429.1	54.8	15.5	0.036	—	585.3
105	353.9	34.5	1.32	—	426.9	434.5	54.2	12.7	—	—	581.0
100	357.9	34.7	1.07	—	430.5	440.2	52.8	9.60	—	—	574.6
95	361.7	34.6	0.799	—	433.3	444.8	50.9	7.39	—	—	568.8
90	365.5	34.4	0.479	—	435.7	449.9	48.1	4.97	—	—	561.0
85	369.3	34.0	0.183	—	437.8	453.5	46.4	3.08	—	—	555.5
80	373.1	32.4	0.091	—	438.2	455.8	43.6	1.72	—	—	548.2
75	375.0	30.6	—	—	436.2	456.3	43.1	0.86	—	—	544.6
70	375.8	28.3	—	—	432.4	454.9	43.0	0.37	—	—	542.0
65	375.4	25.1	—	—	425.6	451.7	42.7	—	—	—	537.1
60	375.0	20.3	—	—	415.6	448.0	42.2	—	—	—	532.4
55	374.2	14.5	—	—	403.2	447.5	38.8	—	—	—	525.1
50	373.1	7.43	—	—	388.0	449.4	31.0	—	—	—	511.4
45	365.5	1.94	—	—	369.4	454.0	18.4	—	—	—	490.8
40	348.3	0.180	—	—	348.7	451.7	7.26	—	—	—	466.2
35	319.8	—	—	—	319.8	433.3	0.726	—	—	—	434.8
30	274.1	—	—	—	274.1	385.3	—	—	—	—	385.3
25	205.6	—	—	—	205.6	320.3	—	—	—	—	320.3
20	106.6	—	—	—	106.6	207.4	—	—	—	—	207.4
15	7.6	—	—	—	7.6	55.3	—	—	—	—	55.3

The relative shapes agree fairly well with each other, except again in the low-energy region. The results by Adamczyk *et al* (30-1000 eV) are as much as 28% lower than tha present results even though the relative shape differs by about 6%. The results by Nagy *et al* (500-1000 eV) are lower by as much as 28% and the relative shape by about 3%. The measurements by Schram *et al* (500-1000 eV) are lower by about 37% than our results even though the relative shape is in excellent agreement. The results by Stephan *et al* (0-180 eV) are lower by about 20% at 180 eV with percentage deviation increasing as the value of electron impact energy decreases. For Ne^{3+} most of the reported measurements including the present results agree well regarding the relative shape above 300 eV. Below 300 eV the only available results (excluding those of Stephan *et al* (1980) which are available in only a very limited energy range) of Gaudin and Hagemann differ from the present results in the relative shape. As for absolute values, all the earlier results are lower than the present ones ranging from about 30% (Gaudin and Hagemann) to about 50% (Schram *et al*).

The total cross sections for neon are shown in figure 5. They have ben obtained by adding the partial cross sections for the production of Ne^{+}, Ne^{2+} and Ne^{3+} and by taking into account the weighting factors for the various degrees of charges. Below the electron impact energy of 100 eV the present results agree well with those of Rapp and Englander-Golden in their absolute magnitude. However, above the impact energy

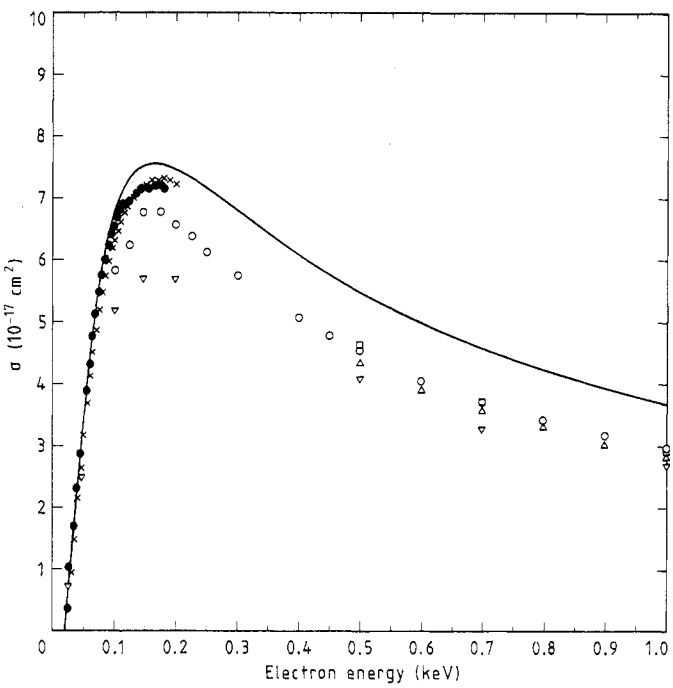

Figure 3. Partial ionisation cross section as a function of electron energy for the process $Ne + e \rightarrow Ne^{+} + 2e$. △, Schram *et al* (1966a, b); ▽, Adamczyk *et al* (1966); ○, Gaudin and Hagemann (1967); □, Nagy *et al* (1980); ●, Stephan *et al* (1980); ×, Wetzel *et al* (1987); full curve, present data. Not included are the data by Bleakney (1930); Stevenson and Hipple (1942) and Ziesel (1965) (see text).

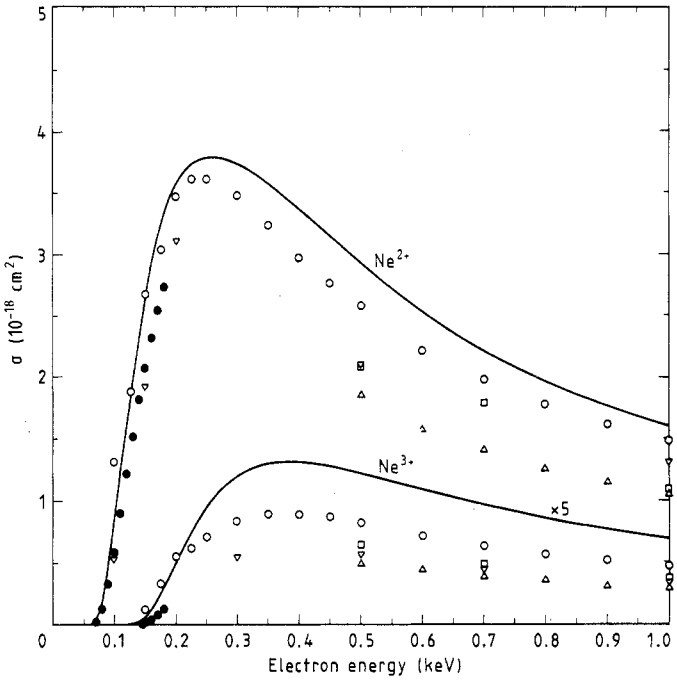

Figure 4. Partial ionisation cross section as a function of electron energy for the processes $Ne+e \rightarrow Ne^{2+}+3e$ and $Ne+e \rightarrow Ne^{3+}+4e$. △, Schram *et al* (1966a, b); ▽, Adamczyk *et al* (1966); ○, Gaudin and Hagemann (1967); □, Nagy *et al* (1980); ●, Stephan *et al* (1980); full curve, present data. As shown in the figure, all the Ne^{3+} data have been multiplied by a factor of 5 for clarity of presentation. Not included are the data by Bleakney (1930), Stevenson and Hipple (1942) and Ziesel (1965) (see text).

of 150 eV the agreement in the absolute mangitude is not so good but the relative shapes agree within 1% with each other. A comparison of the relative shapes of the present results with other results in the 150–1000 eV region gives a deviation of 6% from Schram *et al* (1966a, b), 8% from Gaudin and Hagemann (1967), 13% from Smith (1930) and 0.5% from Rapp and Englander-Golden (1965).

Within the resolution of the electron energy we have not observed any significant structure in the excitation functions of Ne^+, Ne^{2+} or Ne^{3+}.

4.3. Ar

The results for Ar^+, Ar^{2+}, Ar^{3+} and Ar (total ion) are given in figures 6, 7 and 8, respectively, along with other readily available measurements. For Ar^+ (figure 6) the present data and those by Stephan *et al* (1980) (threshold to 180 eV) agree very well with each other. The results of Wetzel *et al* (1987) (0–200 eV) are about 6% higher than those by Gaudin and Hagemann (1967) (100–1000 eV) and are about 13% lower than ours. The relative shapes agree well above 200 eV. The data by Nagy *et al* (1980) (500–1000 eV) agree well with the present results (within 2%) both in relative shape and absolute magnitude. The measurements of Schram *et al* (1966a, b) (500–1000 eV) also agree with the present ones within 4% both in relative shape and the absolute magnitude.

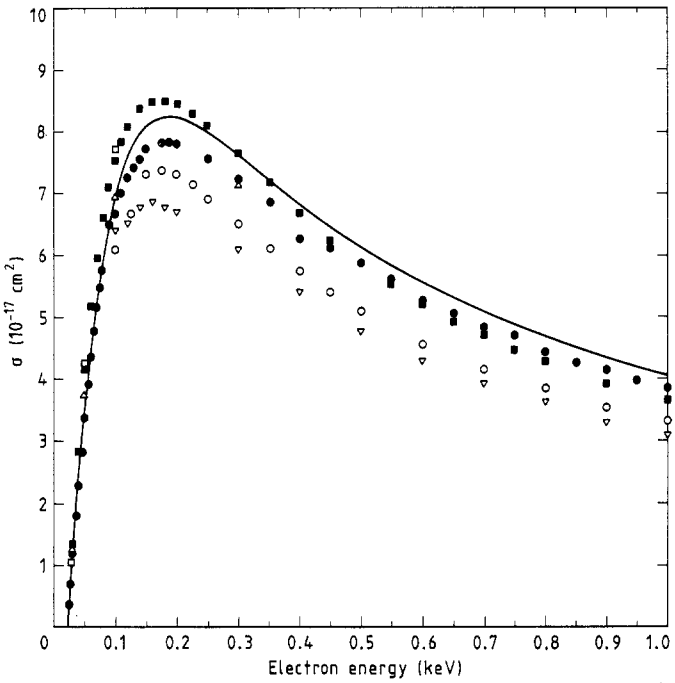

Figure 5. Total ionisation cross section for Ne as a function of electron energy. ■, Smith (1930); □, Asundi and Kurepa (1963); ●, Rapp and Englander-Golden (1965); ▽, Schram *et al* (1965, 1966a, b), ○, Gaudin and Hagemann (1967); △, Fletcher and Cowling (1973); full curve, present data.

The Ar^{2+} data are presented in figure 7 along with other results. Those of Stephan *et al* (1980) are about 26% lower and those of Wetzel *et al* (1987) are about 24% lower than the present ones. The measurements of Gaudin and Hagemann agree well with ours at 1000 eV, but are systematically lower towards the low-energy side. The data of Nagy *et al* (1980) and Schram *et al* (1966a, b) which compare very well with those of Gaudin and Hagemann are also behaving in a similar manner in the energy range of 500 to 1000 eV.

The Ar^{3+} data are shown in figure 7 along with the previous measurements. The results of Fiquet-Fayard (1962) and Okudaira *et al* (1970) have been normalised with ours at 400 eV. The measurements of Stephan *et al* (up to 180 eV) are as much as 45% lower than the present results. The results of Gaudin and Hagemann (1967) seem to fit well with those of Stephan *et al* in the 150–180 eV region and with those of Nagy *et al* (1980) and Schram *et al* in the 500–1000 eV region. However, they fail to show the structure reported by Fiquet-Fayard (1962) and Okudaira *et al* (1970). The present data on Ar^{3+} differ from those of Gaudin and Hagemann both in relative shape and absolute magnitude. The data of Schram *et al* (1966a, b) differ from ours by 30% in absolute values, but agrees within 4% in relative shape. The results of Nagy *et al* are as much as 35% lower than ours at 1000 eV with the relative shape differing by about 10%. The relative shape reported by Fiquet-Fayard, even though it differs from ours by about 8% at 200 eV, clearly supports the double hump we have obtained in our data. This hump is also supported by Okudaira *et al* (1970). However, they differ from us by a relatively sharp decrease in cross section values towards the 1000 eV region.

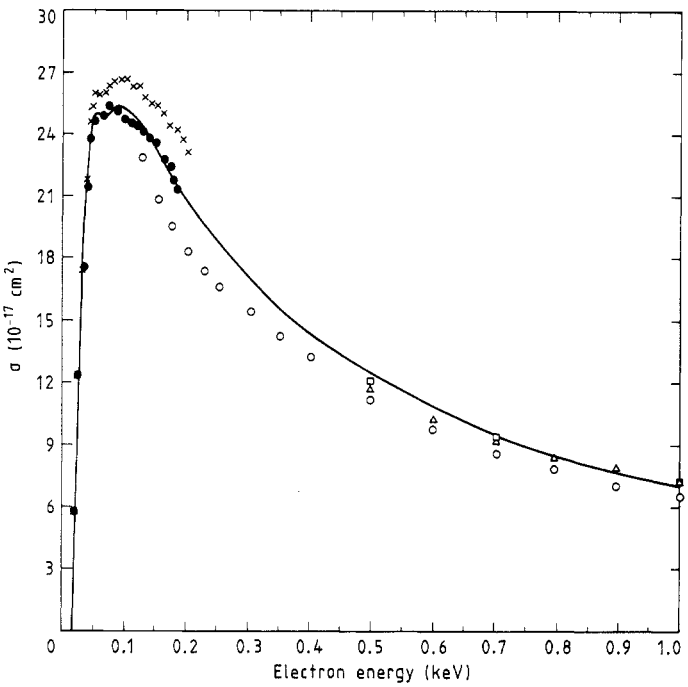

Figure 6. Partial ionisation cross section as a function of electron energy for the process $Ar + e \rightarrow Ar^+ + 2e$. △, Schram *et al* (1966a, b); ○, Gaudin and Hagemann (1967); □, Nagy *et al* (1980); ●, Stephan *et al* (1980); ×, Wetzel *et al* (1987); full curve, present data. Not included are the data by Bleakney (1930); Fox (1960); Crowe *et al* (1972) and Mathur and Badrinathan (1984) (see text).

The total ion data for argon are shown in figure 8. They agree with those published by Rapp and Englander-Golden (1965) to within 3% from threshold to 600 eV. Beyond 600 eV the present data are about 9% lower than those of Rapp and Englander-Golden. The results by Wetzel *et al* (1987) are about 7% higher than ours. Kurepa *et al* (1974) are in excellent agreement with ours. The results of Schram *et al* and Gaudin and Hagemann (1967) are consistently lower in the entire energy range. However, towards high energies Schram *et al* agree better with the present results.

We also confirm the structure below 100 eV in Ar^+ reported by Okudaira *et al* (1970) and Crowe *et al* (1972). This structure was subsequently confirmed by Mathur and Badrinathan (1984), Stephan *et al* (1980) and Wetzel *et al*(1986). The structure that we observe is more similar to that reported by the last two authors whereas the first peak at 50 eV is lower in height compared with the broader peak at 90 eV. This structure was studied in detail by Crowe *et al* (1972) and they concluded that it is due to the autoionisation of the $3s3p^6 4p$ and $3s3p^6 3d$ states of Ar.

No structure has been observed in the past in the excitation function of Ar^{2+} up to 1000 eV. Our results also do not show any special features except that in the present data there is a pronounced enhancement of the peak at 110 eV.

In the case of Ar^{3+} the observed double hump has already been explained by Fiquet-Fayard and Lahmani (1962) as due to an Auger process of the type $A^+_{L_1} \rightarrow A^{2+}_{L_{2,3}M_1} \rightarrow A^{3+}_{M_1M_1M_{2,3}}$ give rise to the Ar^{3+} ions. The first hump centred around 180 eV is due to direct multiple ionisation and the second broad hump which has its onset at about 250 eV is due to the Auger process.

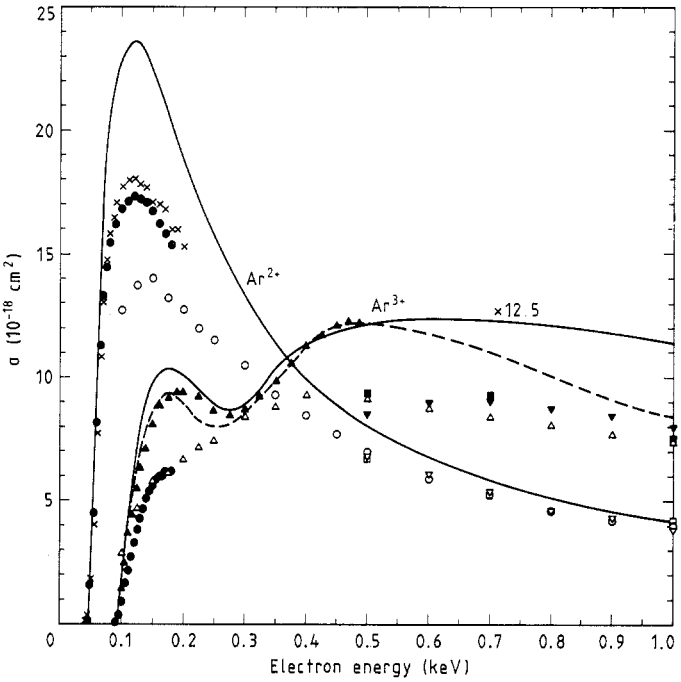

Figure 7. Partial ionisation cross section as a function of electron energy for the processes $Ar + e \rightarrow Ar^{2+} + 3e$ and $Ar + e \rightarrow Ar^{3+} + 4e$. Ar^{2+}: ▽, Schram *et al* (1966a, b); ○, Gaudin and Hagemann (1967); □, Nagy *et al* (1980); ●, Stephan *et al* (1980); ×, Wetzel *et al* (1987); full curve, present data. Ar^{3+}: ▲, Fiquet Fayard (1962); ▼, Schram *et al* (1966a, b); △, Gaudin and Hagemann (1967); broken curve, Okudaira *et al* (1970); ■, Nagy *et al* (1980); ●, Stephan *et al* (1980); full curve, present data. As shown in the figure, all the Ar^{3+} data have been multiplied by a factor of 12.5 for the purpose of clarity of presentation. Not included are the data by Bleakney (1930), Fox (1960), Crowe *et al* (1972) and Mathur and Badrinathan (1984) (see text).

4.4. Kr

The results of the ionisation of Kr are presented in figures 9, 10 and 11 along with the previously published data. For Kr^+ (figure 9) there is no single absolute measurement which covers the entire energy region from threshold to 1000 eV. Indeed, from 200 to 500 eV there are no measurements at all. The two sets of low-energy data by Wetzel *et al* (1987) and Stephan *et al* (1980) compare very well with the present results. Wetzel *et al* have attributed their higher values towards 200 eV to possible systematic errors in their experiment. From 500–1000 eV the present data are in fair agreement with those by Schram *et al* (1966a, b) with the latter being lower by about 6% at 500 eV. The relative shapes agree within 3%. The results by Nagy *et al* (1980) are about 15% higher than ours at 500 eV and the relative shape differs by about 11%.

In the case of Kr^{2+} (figure 9) again there is no earlier measurement in the 200–500 eV range. Our data deviate by about 10% at the peak at about 100 eV from those of Wetzel *et al* (1987) and Stephan *et al* (1980). At 500 eV, the cross section published by Nagy *et al* is 16% lower and that by Schram *et al* is 13% higher than ours. Our

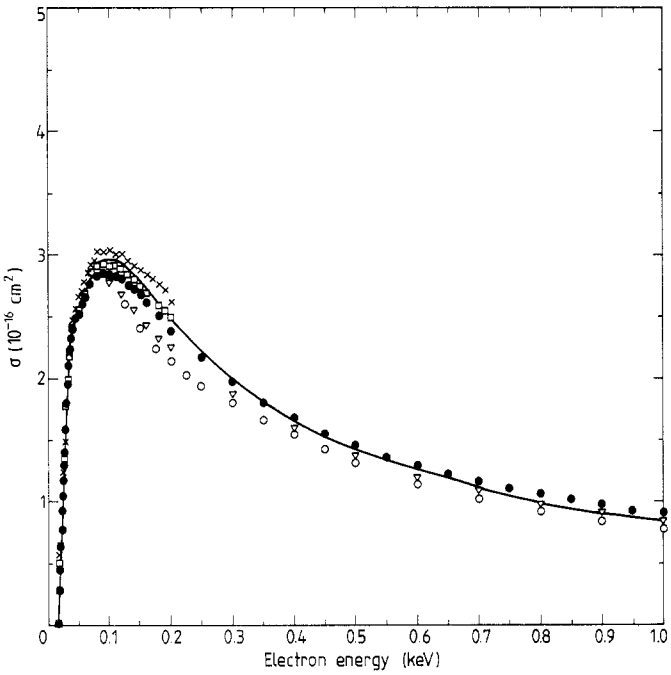

Figure 8. Total ionisation cross section for Ar as a function of electron energy. ●, Rapp and Englander-Golden (1965); ▽, Schram *et al* (1965, 1966a, b); ○, Gaudin and Hagemann (1967); □, Kurepa *et al* (1974); ×, Wetzel *et al* (1987); full curve, present data. Not included are the data by Smith (1930), Tozer and Craggs (1960), Asundi and Kurepa (1963), Srinivasan and Rees (1967) and Fletcher and Cowling (1973) (see text).

relative shape in the 500–1000 eV region differs from the former by about 7% and from the latter by 19%.

For Kr^{3+} (figure 10) our measurements are higher by about 38% compared with those by Stephan *et al* (1980) and about 30% higher than those by Wetzel *et al* (1987) below the electron impact energy of 200 eV and (at 500 eV) 32% higher than that by Nagy *et al* (1980) and 12% higher than that by Schram *et al* (1966a, b).

For Kr^{4+} (figure 10) the measurements have been reported by Stephan *et al* (1980) from threshold to 180 eV and by Schram *et al* (1966a, b) from 500 to 1000 eV. The present results are higher than Stephan *et al*'s measurement by about 40% in the high electron impact energy region. The agreement with those by Schram *et al* is also poor both in the shape and absolute magnitude. Schram *et al*'s results are lower with a maximum deviation at 1000 eV (about 36%). Their relative shape differs by about 22%.

The total ionisation data for krypton are presented in figure 11. The various measurements are in good agreement with each other and thus provide an added confidence in the values of our partial cross sections.

Unlike the case of Ar, and as we shall see for Xe, the presence of structure in the ionisation cross sections of Kr are not very evident even though the data by Ziesel (1967) support some structure at 60 and 100 eV. We have not been able to observe the step-like enhancement in the cross section for Kr^+ at about 28 eV as reported earlier by Mathur and Badrinathan (1984). Valin and Marmet (1975) have carried out a

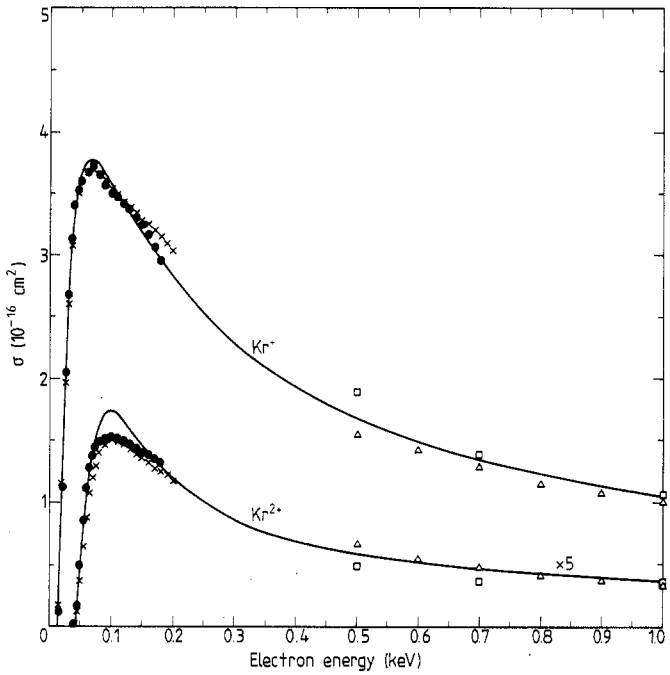

Figure 9. Partial ionisation cross section as a function of electron energy for the processes $Kr+e \rightarrow Kr^+ + 2e$ and $Kr+e \rightarrow Kr^{2+} + 3e$. △, Schram *et al* (1966a, b); ●, Stephan *et al* (1980); □, Nagy *et al* (1980); ×, Wetzel *et al* (1987); full curve, present data. The Kr^{2+} data have been multiplied by a factor of 5 for clarity of presentation. Not included are the data by Tate and Smith (1934), Fox (1960), Ziesel (1967) and Mathur and Badrinathan (1984) (see text).

detailed study of the electron impact ionisation in Kr from 22 to 32 eV. They have observed a number of structures in this energy range after processing the data collected for a long period of time. Their original data show that these structures, even though present, are too small to be seen directly in the present measurements. Fox (1960) has reported some structure in the Kr^+ ionisation curve around 200 eV which seems to be due to instrumental errors.

In the case of Kr^{2+}, except for Fox (1960), nobody has reported any deviation from the otherwise smooth nature of the curve up to 1000 eV. The ionisation efficiency curve given by Fox shows the possibility of some structure at about 200 eV which again could be attributed to the instrumental error which his measurements have been found to be suffering from. The present results also show the absence of any structure in Kr^{2+} up to 1000 eV.

Mathur and Badrinathan (1984) have observed a step-like enhancement in the excitation function of Kr^{3+} in the region of 95 eV and have attributed it to the onset of ionisation of a 3d electron whose binding energy is 93.82 eV. The slight bend in the curve we measured at this energy seems to support this observation. The data by Ziesel (1967) also show similar behaviour. An additional structure has been found in Kr^{3+} at about 140 eV as seen in the results by Ziesel (1967), Stephan *et al* (1980) and Wetzel *et al* (1987). In the present work such a structure could be seen (even though it is very weak). This can be attributed to the onset of the $3d^9 4s^1$ threshold.

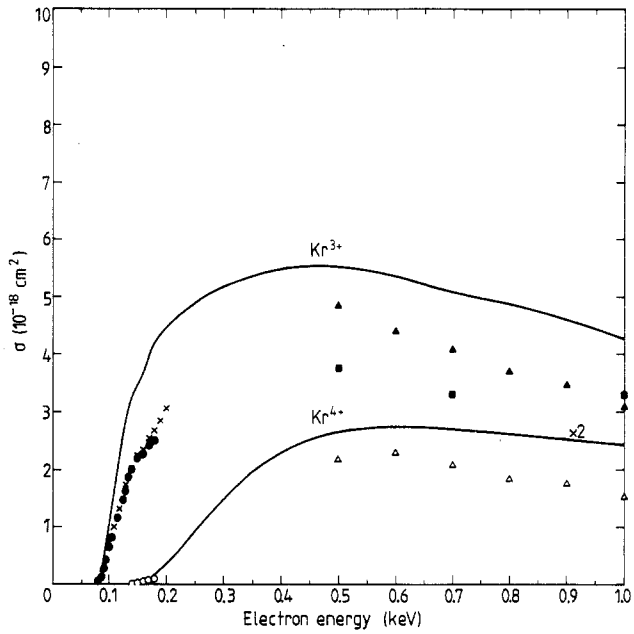

Figure 10. Partial ionisation cross section as a function of electron energy for the processes $Kr + e \rightarrow Kr^{3+} + 4e$ and $Kr^{+} + e \rightarrow Kr^{4+} + 5e$. Kr^{3+}: ▲, Schram *et al* (1966a, b); ■, Nagy *et al* (1980); ●, Stephan *et al* (1980); ×, Wetzel *et al* (1987); full curve, present data. Not included are the data by Tate and Smith (1934), Fox (1960), Ziesel (1967) and Mathur and Bardinathan (1984) (see text). Kr^{4+}: △, Schram *et al* (1966a, b); ○, Stephan *et al* (1980); full curves, present data. The Kr^{4+} data have been multiplied by a factor of 2 for clarity of presentation. Not included are the data by Tate and Smith (1934), Fox (1960) and Ziesel (1967) (see text).

The Kr^{4+} excitation function does not exhibit any special feature. As in the case of Ar, the production of Kr^{3+} and Kr^{4+} is dominated by Auger processes (see Ziesel 1967).

4.5. Xe

The data on Xe^{+} are shown in figure 12 along with other measurements which report the absolute values of cross sections. At low energies the present data seem to be in good agreement with those of Stephan *et al* (1980) except for the difference in height of the first peak. The data by Wetzel *et al* (1987) are about 12% higher near the peak. The results by Schram *et al* (1966a, b) agree very well with the present results from 800 to 1000 eV but are higher by about 7% in the 500–700 eV range. Nagy *et al* (1980) agree closely with us at 500 eV but differ by about 14% at 1000 eV which results in about 16% deviation in the relative shape.

The Xe^{2+} data are also presented in figure 12. The data are higher than those of Stephan *et al* by 23% and those of Wetzel *et al* by 16%. In the 500–1000 eV range the data are in good agreement with those of Schram *et al* both in relative shape and absolute magnitude. The results by Nagy *et al* seem to differ by about 18% in absolute magnitude at 700 eV, and the relative shape varies by about 13%.

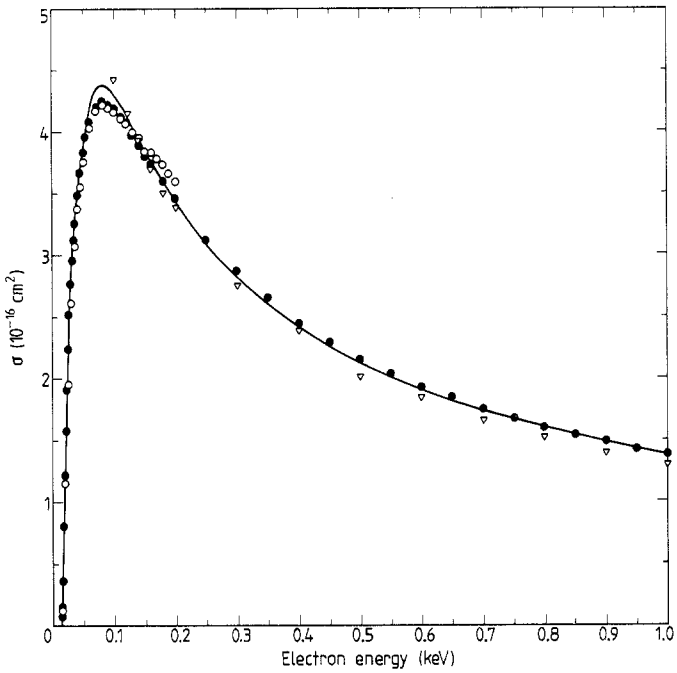

Figure 11. Total ionisation cross section for Kr as a function of electron energy. ▽, Schram *et al* (1965); ●, Rapp and Englander-Golden (1965); ○, Wetzel *et al* (1987); full curve, present data. Not included are the data by Tozer and Craggs (1960) and Asundi and Kurepa (1963) (see text).

The Xe^{3+} data (figure 13) are higher than all the previous measurements which cover the electron impact energy range from 0 to 180 eV. Even though the relative shape agrees fairly well with those given by Wetzel *et al* (1987) and Stephan *et al* (1980) they are about 22 and 33%, respectively, lower than the present results. At higher energies (500 eV and above) the results of Nagy *et al* are lower by 28% with the relative shape differing by about 10%. The results of Schram *et al* (1966a, b) are different from the present results by as much as 30% in absolute magnitude and 8% in the relative shape.

Apart from Schram *et al* there has not been any absolute measurement reported on Xe^{4+} and Xe^{5+}. Our values for both Xe^{4+} and Xe^{5+} are about twice those reported by Schram *et al.* The relative shape of Xe^{4+} seems to differ by about 14% and that of Xe^{5+} is in very good agreement with the present results.

The total ionisation cross section of Xe is given in figure 14. Even though the Xe^{+}data were obtained by normalisation with the data of Rapp and Englander-Golden at 30 eV, the total cross section shows an overall increase of about 10% at higher energies when compared with Rapp and Englander-Golden. This is about 3% higher than the uncertainty due to the normalisation procedure and the probable error in the relative shape. We find that at higher energies our results are in better agreement with Schram *et al* (1965, 1966a, b). The recent measurements of Wetzel *et al* (1987) are in good agreement with the present results within the combined uncertainty in the two measurements.

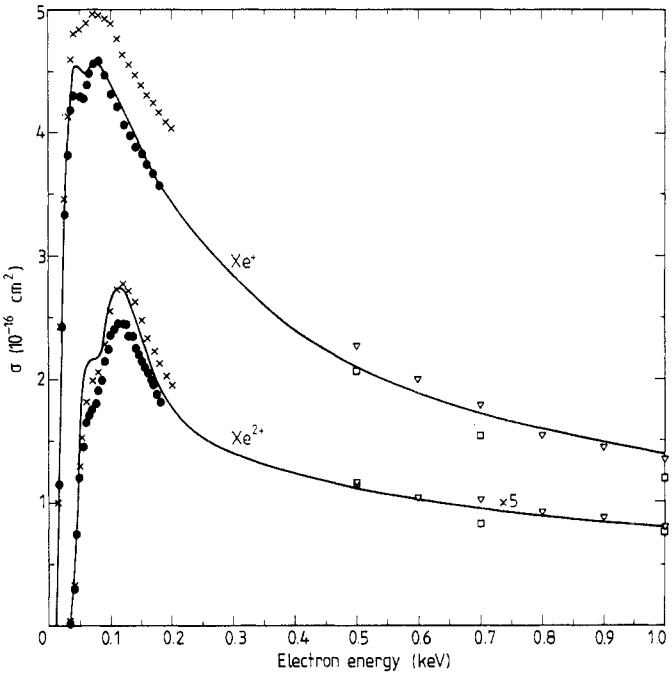

Figure 12. Partial ionisation cross section as a function of electron energy for the processes $Xe + e \rightarrow Xe^+ + 2e$ and $Xe + e \rightarrow Xe^{2+} + 3e$. ▽, Schram *et al* (1966a, b); □, Nagy *et al* (1980); ●, Stephan and Märk (1984); ×, Wetzel *et al* (1987); full curve, present data. The Xe^{2+} data have been multiplied by a factor of 5 for clarity of presentation. Not included in the figure are the data by Tate and Smith (1934), Fox (1959) and Mathur and Badrinathan (1986) (see text).

The double peak observed in Xe^+ is similar to that in Ar^+. The present data show a peak at 42 eV, a valley at 55 eV and a broader peak at 80 eV. The data by Stephan *et al* and Wetzel *et al* also show the same behaviour even though the valley is not so apparent. The data by Mathur and Badrinathan (1984) show the first peak at 42 eV, the valley at 52 eV and the broader peak at 95 eV. Mathur and Badrinathan have tried to explain the structure in Xe^+ as due to the collective nature of the 4d electrons resulting in *intershell* interactions giving rise to transfer of excitation energy from the 4d to the 5p orbital. The calculations by Amusia *et al* (1971) using a plasma-type model show such a behaviour.

The Xe^{2+} data show a step at about 65 eV followed by a peak at about 115 eV. The onset of the peak at about 70 eV fairly matches with the threshold for the ejection of a 4d electron (67.55 eV). The photoionisation data (Berkowitz 1979) show that the ejection of a 4d electron primarily results in the formation of Xe^{2+}. Our data show a change in the smooth ionisation curve which is probably due to the onset of another inner-shell ionisation at about 300 eV.

Xe^{3+}, Xe^{4+} and Xe^{5+} all show some broad structures between 300 and 700 eV. The cause of the structure in Xe^{3+} and Xe^{4+} starting from about 300 eV could be attributed to the inner-shell ionisation which gives rise to the broad hump in Xe^{2+} in the same energy range.

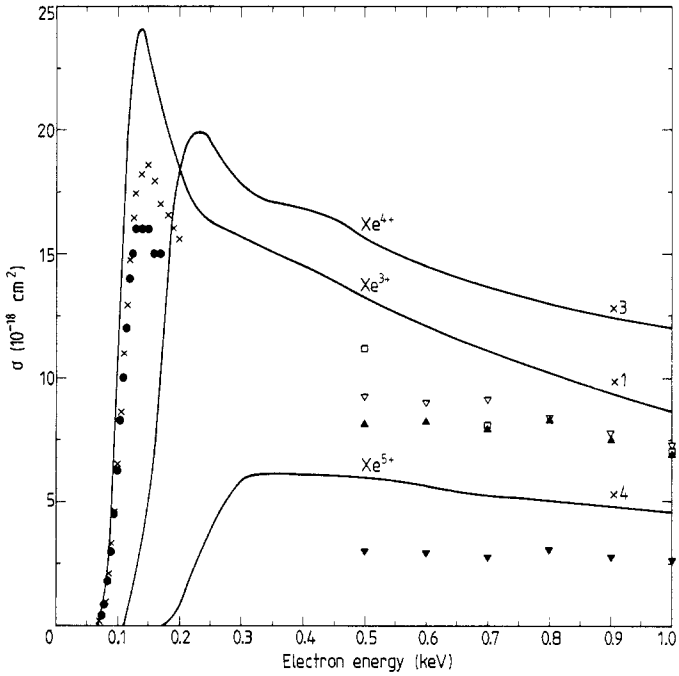

Figure 13. Partial ionisation cross section as a function of electron energy for the processes $Xe+e \rightarrow Xe^{3+}+4e$, $Xe+e \rightarrow Xe^{4+}+5e$ and $Xe+e \rightarrow Xe^{5+}+6e$. Xe^{3+}: ▽, Schram *et al* (1966a, b); □, Nagy *et al* (1980); ●, Stephan and Märk (1984); ×, Wetzel *et al* (1987); full curve, present data. Xe^{4+}: ▲, Schram *et al* (1966a, b); full curve, present data. The data have been multiplied by a factor of 3 for clarity of presentation. Not included in the figure are the data by Tate and Smith (1934) and Fox (1959) (see text). Xe^{5+}: ▼, Schram *et al* (1966a, b); full curve, present data. The data have been multiplied by a factor of 4. Not included in the figure are the data by Tate and Smith (1934) and Fox (1959) (see text).

5. Discussion

We have obtained relatively higher values for the partial ionisation cross sections for the multiply charged species as compared with various other measurements. We believe these numbers to be correct since we have carefully carried out a specific mass transmission calibration procedure, employed a pulsed electron beam and ion extraction technique and kept both the electron current and the gas pressure very low.

A review of the previous measurements shows that nobody has used an overall direct calibration procedure as we have. For example, in almost all the cases only indirect methods have been used to show that the mass analyser had 100% transmission or a constant fraction transmission. In some cases the detector was calibrated against a Faraday collector but in others the ions were accelerated to high energy so that the ratio of the intensities of multiply charged ions to the singly charged ions reached a constant value. This does not necessarily eliminate possible systematic errors. Again only indirect methods have been used to show that either complete extraction or a constant fraction extraction (both independent of the mass-to-charge ratios) of the ions from the ionisation region has been achieved.

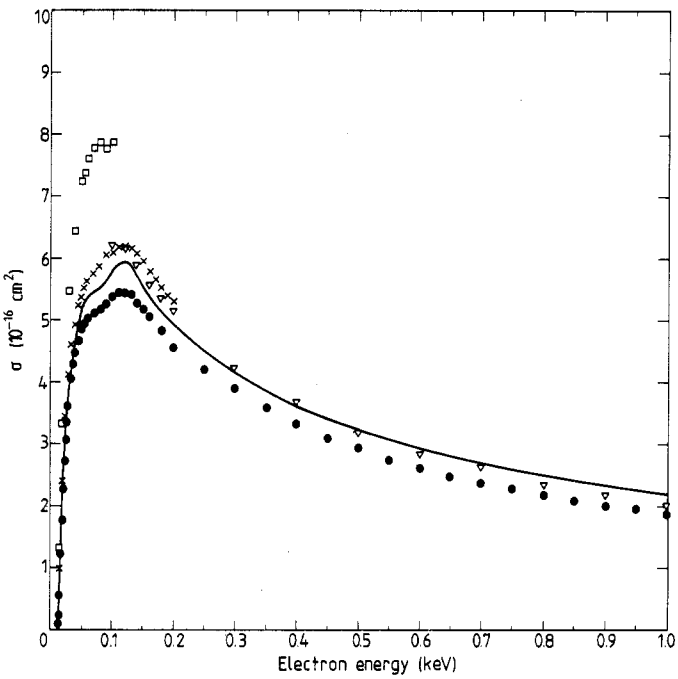

Figure 14. Total ionisation cross section of Xe as a function of electron energy. □, Asundi and Kurepa (1963); ▽, Schram *et al* (1965, 1966a, b); ●, Rapp and Englander-Golden (1965); ×, Wetzel *et al* (1987); full curve, present data. Not included are the data of Tozer and Craggs (1960) (see text).

It is interesting to note that the measurements by Van der Wiel *et al* (1969) and El Sherbini *et al* (1970) from 2-14 keV give higher ratios of the intensities of the multiply charged to singly charged ions than have been reported by both Nagy *et al* (1980) and Schram *et al* (1966a, b) in that energy range. The data are higher by about a factor of 1.5 for 2+ ions and up to a factor of 4 for 6+ ions as compared with Schram's data. Nagy *et al* (1980) and Märk (1981) have considered the results by El Sherbini *et al* (1970) and Van der Wiel *et al* (1969) as unreliable for reasons we fail to understand.

Acknowledgments

The research reported in this paper was carried out at the Jet Propulsion Laboratory and was sponsored by AFOSR and the National Aeronautics and Space Administration. One of us (EK) would like to thank NRC, Washington, DC, for a Resident Research Associateship grant during the course of this work. We are grateful to Mr Charles Thoms for putting together various electronic circuits.

References

Adamczyk B, Boerboom A J H, Schram B L and Kistemaker J 1966 *J. Chem. Phys.* **44** 4640-2
Amusia M Ya, Cherepkov N A and Chernysheva L V 1971 *Sov. Phys.-JETP* **33** 90-6
Asundi R K and Kurepa M V 1963 *J. Electron. Control* **15** 41-50

Bell K L, Gilbody H B, Hughs J G, Kingston A E and Smith F J 1983 *J. Phys. Chem. Ref. Data* **12** 891-916
Berkowitz J 1979 *Photoabsorption, Photoionization and Photoelectron Spectroscopy* (New York: Academic) p 183
Bevington P R 1969 *Data Reduction and Error Analysis for the Physical Sciences* (New York: McGraw-Hill) p 204
Bleakney W 1930 *Phys. Rev.* **36** 1303-8
Bleakney W and Smith L G 1936 *Phys. Rev.* **49** 402
Brinkman R T and Trajmar S 1981 *J. Phys. E: Sci. Instrum.* **14** 245-55
Crowe A, Preston J A and McConkey J W 1972 *J. Chem. Phys.* **57** 1620-5
De Heer F J and Inokuti M 1985 *Electron Impact Ionization* ed T D Märk and G H Dunn (New York: Springer) pp 232-76
El-Sherbini Th M, Van der Wiel M J and De Heer F J 1970 *Physica* **48** 157-64
Fiquet-Fayard F 1962 *J. Chim. Phys.* **59** 439-41
Fiquet-Fayard F and Lahmani M 1962 *J. Chim. Phys.* **59** 1050-5
Fletcher J and Cowling I R 1973 *J. Phys. B: At. Mol. Phys.* L258-61
Foner S N and Nall B H 1961 *Phys. Rev.* **122** 512-24
Fox R E 1959 *Advances in Mass Spectrometry* ed S D Waldron (London: Pergamon) pp 397-412
—— 1960 *J. Chem. Phys.* **33** 200-5
Fox R E, Hickam W M, Grove D J and Kjeldar T Jr 1955 *Rev. Sci. Instrum.* **26** 1101
Gaudin A and Hagemann R 1967 *J. Chim. Phys.* **64** 1209-21
Khakoo M A and Srivastava S K 1984 *J. Phys. E: Sci. Instrum.* **17** 1008-13
Kieffer L J and Dunn G H 1966 *Rev. Mod. Phys.* **38** 1-35
Krishnakumar E and Srivastava S K 1986 *Astrophys. J.* **307** 795-9
Kurepa M V, Čadež I M and Pejčev V M 1974 *Fizika* **6** 185-209
Märk T D 1982 *Beitr. Plasmaphys.* **22** 257-94
—— 1985 *Electron Impact Ionization* ed T D Märk and G H Dunn (New York: Springer) pp 137-97
Mathur D and Badrinathan C 1984 *Int. J. Mass Spectrom. Ion Processes* **57** 167-78
—— 1985 *Int. J. Mass Spectrom. Ion Processes* **68** 9-14
Montague R G, Harrison M F A and Smith A C H 1984 *J. Phys. B: At. Mol. Phys.* **17** 3295-310
Nagy P, Skutlartz A and Schmidt V 1980 *J. Phys. B: At. Mol. Phys.* **13** 1249-67
Okudaira S, Kaneko Y and Kanomata I 1970 *J. Phys. Soc. Japan* **28** 1536-41
Orient O J and Srivastava S K 1983 *J. Chem. Phys.* **78** 2949-52
Rapp D and Englander-Golden P 1965 *J. Chem. Phys.* **43** 1464-79
Schram B L 1966 *Physica* **32** 197-208
Schram B L, Boerboom A J H and Kistemaker J 1966a *Physica* **32** 185-96
Schram B L, De Heer F J, Van Der Wiel M J and Kistemaker J 1965 *Physica* **31** 94-112
Schram B L, Moustafa H R, Schutten J and De Heer F J 1966b *Physica* **32** 734-40
Smith P T 1930 *Phys. Rev.* **36** 1293-302
Srinivasan V and Rees J A 1967 *Brit. J. Appl. Phys.* **18** 59-64
Srivastava S K, Chutjian A and Trajmar S 1975 *J. Chem. Phys.* **63** 2659
Srivastava S K and Nguyen H P 1987 *Jet Propulstion Laboratory Publication No 87-2.*
Stephan K, Helm and Märk T D 1980 *J. Chem. Phys.* **73** 3763-78
Stephan K and Märk T D 1984 *J. Chem. Phys.* **81** 3116-7
Stevenson D P and Hipple J A 1942 *Phys. Rev.* **62** 237-40
Tate J T and Smith P T 1932 *Phys. Rev.* **30** 270-7
—— 1934 *Phys. Rev.* **46** 773-6
Tozer B A and Craggs J D 1960 *J. Electron Control* **8** 103-9
Valin M and Marmet P 1975 *J. Phys. B: At. Mol. Phys.* **8** 2953-67
Van der Wiel M J, El-Sherbini Th M and Vriens L 1969 *Physica* **42** 411-20
Wetzel R C, Baiocchi F A, Hayes T R and Freund R C 1987 *Phys. Rev.* A **35** 559-77
Ziesel J P 1965 *J. Chim. Phys.* **62** 328-35
—— 1967 *J. Chim. Phys.* **64** 695-701